Praseodymium in heavy metal oxyfluoride glass systems

W. A. PISARSKI

University of Silesia, Institute of Materials Science, Katowice, Poland

A new thermally stable glasses based on P_2O_5 – InF_3 and PbF_2 – B_2O_3 containing Pr^{3+} ions were prepared, which belong to wide family of heavy metal oxyfluoride systems. Influence of P_2O_5 content on thermal, structural and optical behavior of multicomponent InF_3 – based glass has been investigated, whereas the second oxyfluoride system in the case of total substitution PbO by PbF_2 has been analyzed. A large value of stability parameter ΔT close to 157^0C was obtained for Pr – doped oxyfluoride glass with 8% of P_2O_5 content. With further increasing P_2O_5 content stability parameter ΔT decreased and several crystalline peaks related to InOF phase appeared, what was stated by X-ray diffraction. Shift of luminescence lines has been observed for both heavy metal oxyfluoride glass systems. However, shift direction depends on kind of additives (oxide or fluoride components) to the basic matrix. Incorporation of P_2O_5 results in shift of red luminescence due to the $^1D_2$ – $^3H_4$ transition of Pr^{3+} ions in direction to longer wavelengths. The opposite situation is observed for glass based on PbF_2 – B_2O_3 emitting reddish–orange light. Substitution PbO by PbF_2 leads to shift of luminescence band in direction to shorter wavelengths.

(Received April 10, 2006; accepted May 18, 2006)

Keywords: Oxyfluoride glasses, Pr^{3+} ions, Glass stability, Luminescence

1. Introduction

Heavy metal oxyfluoride glasses containing rare earth ions are the most important class of the modern advanced materials for application in optoelectronics, which have been extensively studied in recent years. The main disadvantages of fluoride glasses are poor chemical and mechanical stability and easy crystallization. In contrast to simple oxide or fluoride glasses, some advantages have been observed in mixed oxyfluoride systems, which combined the excellent optical properties of rare earth ions in fluoride host with simultaneously large chemical stability and mechanical property of oxide glasses. Several reports on the oxyfluoride glass systems in different chemical compositions have been known in literature. One of them is phosphate fluoride glass containing P_2O_5 and CaF_2 [1] as well as lead fluoroborate glass [2], which have been investigated using spectroscopic methods.

Praseodymium – doped crystals and glasses have proved to be effective for several applications in optical devices as blue up-converters ($^3P_0$ – $^3H_4$) and solid-state lasers emitting visible ($^1D_2$ – $^3H_4$) or near-infrared light ($^1G_4$ – $^3H_5$), respectively. The latter plays the role as efficient amplifier working around 1.3μm requested for optical telecommunication systems. Especially, Pr^{3+} ions in a great number of optical materials like crystalline compounds [3] as well as heavy metal oxide and fluoride glasses [4] exhibit a prominent red luminescence from the $^1D_2$ excited state. In contrast to them, more intensive visible luminescence due to $^3P_0$ – $^3F_2$ transition than $^1D_2$ – $3H_4$ one is observed for Pr^{3+} ions in polymeric (PMMA) materials [5]. Recently, chalcogenide glass – polymer composite materials containing Pr^{3+} ions were prepared [6], which can be interesting from the optical point of view.

Recently, rare earth doped fluoride and oxide glasses based on InF_3 [7-11] and PbO – B_2O_3 [12-16] were investigated. Presented work deals with thermal, structural and optical investigations of Pr^{3+} ions in two different heavy metal oxyfluoride glassy matrices based on P_2O_5 – InF_3 and PbF_2 – B_2O_3. Both optical systems have been investigated using DSC, XRD, FT-IR and photoluminescence spectroscopy.

2. Experimental details

Oxyfluoride glasses in $(72–x)PbO–xPbF_2–18B_2O_3–6Al_2O_3–3WO_3–1Pr_2O_3$ (x = 0 ÷ 72 wt%) system referred as $xPbF_2$ – PBAW:Pr and $44InF_3–14ZnF_2–(19-x)BaF_2–xP_2O_5–17SrF_2–3GaF_3–2LaF_3–1PrF_3$ (x = 0 ÷ 16 wt%) system referred as xP_2O_5 – IZBSGL:Pr were prepared. For both systems, anhydrous oxides and fluorides (99.99% purity, Aldrich) were used as a starting materials and a homogeneous mixture was heated in a protective atmosphere of dried argon. Glasses were melted at 850^0C in Pt crucibles, then poured into preheated copper moulds and annealed below the glass transition temperature. After this procedure, the samples were slowly cooled to the room temperature.

The glass samples were characterized by a Perkin Elmer differential scanning calorymeter (DSC) and INEL diffractometer (XRD). The DSC curves were measured with a heating rate of 10deg/min. The X-ray diffraction analysis was carried out with Cu Kα radiation in 2θ ranges 0^0 to 120^0. The IR transmission spectra in range of 400 - 4000 cm^{-1} were taken on BIO-RAD FT-IR spectrometer using the standard KBr pellet disc technique. The samples has been excited by a Continuum Surelite Optical Parametric Oscillator (OPO), pumped by a third harmonic of a Nd:YAG laser. The luminescence was dispersed by a 1-meter double grating monochromator and detected with a photomultiplier with S-20 spectral response. The luminescence spectra were recorded using a Stanford SRS 250 boxcar integrator controlled by a computer. Luminescence decay curves were recorded and stored by a

Tektronix TDS 3052 oscilloscope. All measurements were carried out at room temperature.

3. Results and discussion

3.1 P_2O_5–InF_3–ZnF_2–BaF_2–SrF_2–GaF_3–LaF_3–PrF_3 glasses

Thermal properties of xP_2O_5 – IZBSGL:Pr oxyfluoride glasses containing different concentration of P_2O_5 have been examined. Fig. 1 shows DSC curves recorded for glasses based on P_2O_5 – InF_3 containing Pr^{3+} ions. From DSC curves characteristic temperatures such as glass transition temperature T_g, crystallization onset T_x and maximum of the crystallization peak T_p were obtained, from which stability factor ΔT defined as difference between glass transition temperature T_g and crystallization onset T_x, was calculated. This parameter plays an important role in manufacturing of the optical fibers.
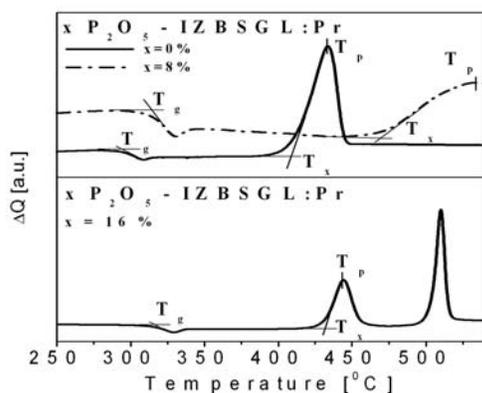
Fig. 1. DSC curves recorded for Pr – doped glasses based on P_2O_5 – InF_3.

Rare earth – doped fluoride glass has been formed in many elements systems, but only a few numbers of them can be considered as stable and suitable for optical devices. Unfortunately, one of the main disadvantages to application is relatively low thermal stability and easy crystallization during melting and forming. From literature concerning data about preparation of fluoride glass fibers it is known, that fiber drawing is possible when value of ΔT is higher than 100^0C. This parameter usually does not exceed 100^0C in ternary InF_3–ZnF_2–BaF_2–SrF_2 (IZBS) fluoride glasses. However, further optimization was achieved in IZBS basic system using different fluorides as stabilizing additives to decrease devitrification rate. Increasing the number of components may enhance glass-forming ability. Thus, it is possible to obtain thermally stable fluoride glasses with relatively high ΔT factors in the multicomponent InF_3 – based systems. The values of ΔT close to 108 °C with GaF_3 [17], 117 °C with LiF [18] and 118 °C with GaF_3 and LaF_3 [19] components in the InF_3 – based glasses were obtained. The addition of new components to the base glass is still under the test because of changes of the glass composition as well as the relative ratios of the existing components drastically influence on

thermal and optical properties. For that reason, P_2O_5 as a well-known glass-former and stabilizing component was added to the fluoride matrix. For Pr–doped fluoroindate glass without P_2O_5 thermal stability parameter ΔT is found to be 116 °C. The best value of ΔT close to 157 °C was obtained for mixed oxyfluoride system with 8% of P_2O_5 content. Further addition of P_2O_5 leads to decrease ΔT factor and partial crystallization of the investigated oxyfluoride glass system. It results in an additional second exothermic peak observed for mixed oxyfluoride glass with 16% of P_2O_5 content and suggests that crystallization process takes place. It is consistent with XRD results.
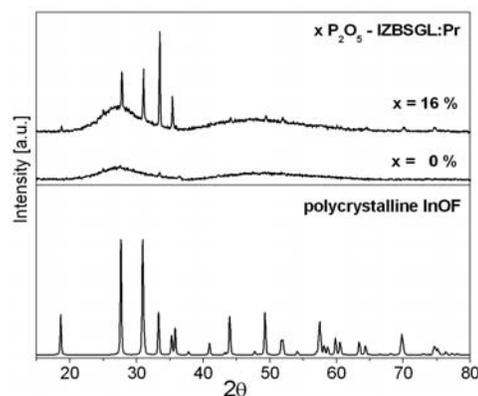
Fig. 2. X-ray diffraction patterns for Pr – doped glasses based on P_2O_5 – InF_3.

Fig. 2 shows the X-ray diffraction patterns obtained for samples without and with 16% of P_2O_5 content, respectively. The XRD patterns of samples without and with P_2O_5 (up to 12%) display two broad peaks corresponding to remaining amorphous phases. Glass tendency towards crystallization increases with further increasing oxide component and several diffraction lines due to the crystalline phases are observed for sample with 16% of P_2O_5 content. Phase identification reveals, that crystalline peaks can be related to the InOF phase.
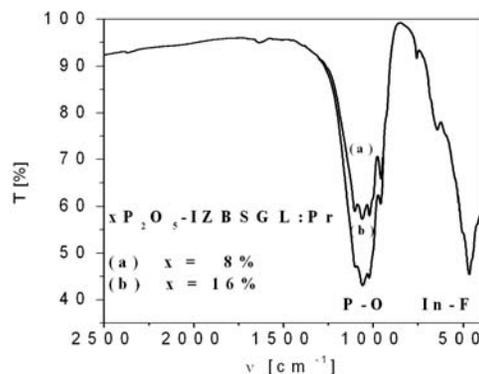
Fig. 3. FT-IR transmission spectra recorded for Pr – doped glasses based on P_2O_5 – InF_3.

It also corroborates results obtained from FT-IR transmission measurements (Fig. 3), where lines

associated with non-bridging P-O vibrations are shifted in direction of lower frequencies with increasing P_2O_5 content (red shift). It indicates that phosphate group was able to bridge octahedral $[InF_6]$ group. At consequence, InOF phase is formed, which was evidenced using X-ray diffraction analysis for sample with 16% of P_2O_5. Two intense bands associated with In-F and P-O vibrations are observed for Pr – doped oxyfluoride glasses in the IR transmission spectra. The first band existing at 468 cm^{-1} is assigned to the ν_1 (A_{1g}) symmetric vibration of the octahedral $[InF_6]$ group. The second broad band consists of four lines appearing at 957, 1021, 1061 and 1103 cm^{-1}, which are assigned to the P-O symmetric (ν_s) and asymmetric (ν_{as}) stretching vibrations. The intensity of these lines increases with increasing of P_2O_5 content. Detailed information about assignment of infrared bands associated with P-O vibrations can be found in [1, 20].

Fig. 4 shows luminescence registered for Pr^{3+} ions in fluoride and oxyfluoride InF_3 – based glass. Luminescence from both $^3P_0$ and $^1D_2$ excited levels are observed for fluoride and oxyfluoride systems under excitation of $^3P_2$ level of Pr^{+3} ions. Energy gap between $^3P_0$ level and the next lower $^1D_2$ level is found to be 3900cm^{-1}. Using the measured and calculated radiative lifetimes for the $^3P_0$ level in case of low Pr^{+3} concentration and phonon energy of the host ($\hbar\nu\sim500$ cm^{-1}), the non-radiative transition rate W_{nr} can be calculated. The W_{nr} value due to multiphonon relaxation process determined in [21] for InF_3 – based glass is close to 2.47×10^4 s^{-1}, which indicates that radiative and non-radiative transitions from the $^3P_0$ level take place. The $^3P_0$ level can populate quite efficiently $^1D_2$ level. From this point of view it is possible to observe emission from $^3P_0$ and $^1D_2$ levels in this spectral range. Thus two stronger asymmetric and less intense emission bands were recorded at 603, 616 and 636 nm, which correspond to the $^1D_2$ - $^3H_4$, $^3P_0$ - $^3H_6$ and $^3P_0$ - $^3F_2$ transitions, respectively. These luminescence lines are shifted to longer wavelengths, when P_2O_5 was introduced to the InF_3 – based fluoride glass.
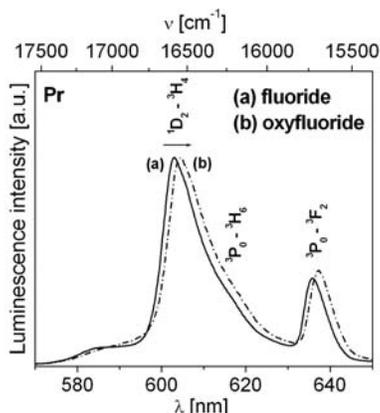
Fig. 4. Luminescence spectra recorded for Pr^{3+} ions in fluoride and oxyfluoride InF_3 – based glasses.

3.2 PbF_2–PbO–B_2O_3–Al_2O_3–WO_3–Pr_2O_3 glasses

Thermal properties of glasses based on PbF_2 – B_2O_3 containing Pr^{3+} ions have been analyzed. Influence of PbF_2

on thermal behavior has been investigated using differential scanning calorimetry (DSC). Figure 5 presents DSC curves for oxyfluoride glasses with low (9%), middle (36%) and high (72%) PbF_2 concentrations. The glass transition temperature was evaluated, but no obvious crystallization peak was detected in the limited range of DSC – 600 ^{0}C. Inset shows evolution of glass transition temperature T_g as a function of PbF_2 concentration (0 ÷ 72% wt). It is clearly seen, that glass transition temperature slightly decreases with increasing PbF_2 concentration in glass composition.
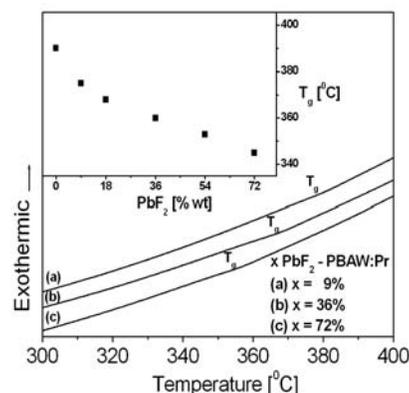
Fig. 5. DSC curves recorded for Pr – doped glasses based on PbF_2 – B_2O_3.

Dependently on PbF_2 concentration, the glass transition temperatures are located in 350–375^{0}C ranges, which is in a good agreement with results obtained for similar Sm^{3+} or Dy^{3+} doped glasses in B_2O_3 – ZnO – PbO system [22].

The value of T_g strongly depends on O/F ratio in glass composition. Introduction of the oxide component such as P_2O_5 to the InF_3 – based fluoride matrix induces an increase of glass transition temperature, which is attributed to the formation of stronger chemical bonds (see chapter 3.1, Fig. 1). The opposite effect has been observed for glass based on PbF_2 – B_2O_3. Firstly, as the PbF_2 content increases the T_g values decrease rapidly suggesting that the PbF_2 content acts as a network modifier. Secondly, the covalency of the Pb – F bond is smaller than that of the Pb – O bond because of the larger difference of electronegativity between cation and anion ions. It is expected that the influence of the Pb – F bond on the local ligand environments around Pr^{3+} ions increase with increasing of PbF_2 concentration. Consequently, the covalency of the Pr – O/F bond decreases. Therefore, it suggests based on the observed evolution of T_g that the introduction of fluoride component decreases the strength of the average chemical bond and/or produces a less linked or interconnected glass network.

Fig. 6 presents FT-IR transmission spectra recorded for Pr – doped glasses based on PbF_2–B_2O_3. The IR cut-off wavelength increases from 7.2 μm to 7.75 μm, when PbO was totally substituted by PbF_2 in glass composition. Addition of heavy metal fluoride component to the oxide matrix increases its IR cut-off wavelength. Both values for our borate matrix with heavy metal oxide (PbO) or fluoride (PbF_2) components are higher in comparison to

traditional borate glasses (~ 3 μm), but considerably smaller than that one obtained for fluoride system (above 20 μm) based on InF_3 [19].
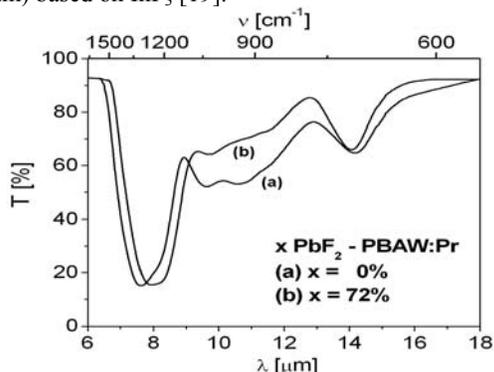
Fig. 6. FT-IR transmission spectra recorded for Pr – doped glasses based on $PbF_2 – B_2O_3$.

The infrared bands due to the B–O vibrations have been observed in 1500–600cm^{-1} spectral ranges. Three characteristic groups of bands are due to BO_3 bending (650–700 cm^{-1}) and stretching vibrations of tetrahedral BO_4 (850–1050 cm^{-1}) and trigonal BO_3 (~ 1300 cm^{-1}) units, respectively. Two important effects associated with total substitution of PbO by PbF_2 can be observed. Firstly, these bands are shifted to the lower frequency region (longer wavelengths). Secondly, the intensity of the infrared band related to the BO_4 units decreases, when PbO was replaced by PbF_2 in glass composition. The PbO_4 units bridge preferentially rather to BO_3 groups than BO_4 ones. The fluorine atoms added to the glass network start to reduce BO_4 units. Thus, the intensity of infrared band associated with BO_4 group decreases as clearly seen in Fig. 6. The opposite effect was observed for Sm – doped lead fluoroborate glass in the case of BO_4 unit formation, when the oxygen atoms added to the oxyfluoride glassy network reduces the effect of fluorine ions in the PbO_4 units [23].
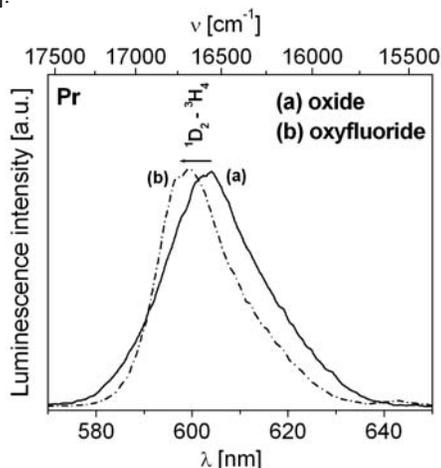
Fig. 7. Luminescence spectra recorded for Pr^{3+} ions in oxide and oxyfluoride lead borate glasses.

In contrast to glass based on $P_2O_5 – InF_3$, quite intense luminescence from the $^1D_2$ state was registered for glass based on $PbF_2 – B_2O_3$ under excitation of the $^3P_2$ level of Pr^{3+} (Fig. 7). Blue shift of luminescence band related to the $^1D_2 – {}^3H_4$ transition of Pr^{3+} ions in oxyfluoride glass is observed in comparison to the oxide one. Excitation energy transfers very fast from $^3P_2$ level via $^3P_1$ level to the $^3P_0$ level by nonradiative relaxation. Energy gap between $^3P_0$ level and the next lower lying $^1D_2$ level is found to be 3800 cm^{-1}. Thus, only three phonons ($\hbar\nu$ = 1260 cm^{-1}) are needed to bridge energy gap. Thus, the $^1D_2$ level is populated quite efficiently by $^3P_0$ level of Pr^{3+} ions.

From the exponential dependence of the multiphonon relaxation rates for rare earth ions in various glasses on the energy gap to the next-lower level, it is clearly seen that W_{nr} value for borate glass is approximately 10^3 times larger than that of fluoride system [24]. Thus, the $^1D_2$ state is populated more efficiently in oxide or oxyfluoride lead borate glasses than fluoroindate ones with or without P_2O_5. At consequence, only luminescence from $^1D_2$ excited state is observed, which corresponds to the $^1D_2 – {}^3H_4$ transition of Pr^{3+} ions. The luminescence band in 570 – 640 nm spectral range due to the $^1D_2 – {}^3H_4$ transition of Pr^{3+} ions is shifted in direction to the shorter wavelengths, when PbO was totally substituted by PbF_2.

Measured (τ_m) and calculated (τ_{rad}) radiative lifetimes of $^1D_2$ excited state of Pr^{3+} ions in oxide and oxyfluoride lead borate glasses have been schematized in Figure 8. Luminescence lifetimes are compared to that ones obtained for fluoride and oxyfluoride InF_3 – based systems. Radiative lifetimes for $^1D_2$ excited state of Pr^{3+} ions in fluoroindate glass [25] and lead borate glass [26] were calculated using Judd-Ofelt theory [27, 28]. Quantum efficiency (η) defined as τ_m / τ_{rad} was calculated. The η value of $^1D_2$ excited state for lead borate glass (η = 14%) is much smaller than that obtained for fluoroindate matrix (η = 88%). It indicates that contribution of nonradiative processes to the excited state relaxation of Pr^{3+} ions in lead borate glasses is significantly higher than fluoroindate ones. At consequence, the mechanism of $^1D_2$ excited state relaxation is quite different in InF_3 – based glass [25] than $PbO-B_2O_3$ based system [26]. Both heavy metal systems have been analyzed as a function of PbF_2 and P_2O_5 content, respectively.
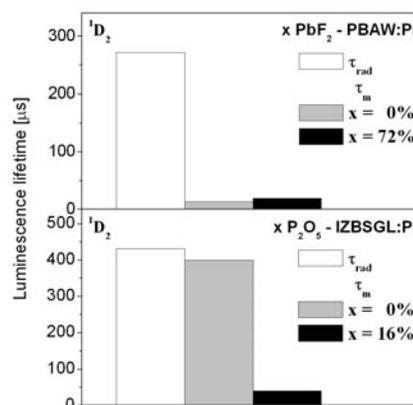
Fig. 8. Influence of PbF_2 and P_2O_5 on luminescence lifetimes for Pr^{3+} ions in oxyfluoride glasses.

It should be noticed that luminescence lifetime for $^1D_2$ state (τ_m = 16.5 μs) of Pr^{3+} ions in highly PbF_2 – concentrated sample (72%) is slightly longer than that one in case of absence PbF_2 (13.5 μs). Both values are similar to that ones obtained for Pr–doped borate crystals [29]. However, the discrepancy between the $^1D_2$ lifetimes of Pr^{3+} ions in fluoroindate glasses without (400 μs) and with (35 μs) P_2O_5 is significant.

4. Conclusions

Thermal, structural and optical properties of Pr^{3+} ions in multicomponent oxyfluoride glass matrices have been investigated. Several transparent oxyfluoride Pr–doped samples were prepared in wide range of PbF_2 concentrations, which indicates that large glass-forming region exists in lead fluoroborate systems. Quite different situation is observed for Pr–doped glasses based on P_2O_5 – InF_3, which relatively quickly and easy crystallized. It results in occurrence of crystalline InOF phase identified using by X-ray diffraction analysis for oxyfluoride sample with 16% of P_2O_5 content. However, it is possible to obtain transparent and thermally stable oxyfluoride glassy samples in narrow range of P_2O_5 concentrations. A large value of stability parameter ΔT close to 157 °C was obtained for sample with 8% of P_2O_5 content.

Luminescence properties of Pr^{3+} ions in both heavy metal oxyfluoride glasses have been compared. Red luminescence corresponding to the $^1D_2$ – $^3H_4$ transition of Pr^{3+} ions in glass based on P_2O_5 – InF_3 is shifted in direction to longer wavelengths. Opposite situation is observed for glass based on PbF_2 – B_2O_3 emitting reddish-orange light, where luminescence band is shifted to shorter wavelengths.

References

[1] N. Vedeanu, O. Cozar, I. Ardelean, B. Lendl, J. Optoelectron. Adv. Mater. **8(1)**, 78 (2006).

[2] J. Pisarska, W. A. Pisarski, J. Optoelectron. Adv. Mater. **7**(5), 2667 (2005).

[3] P. Boutinaud, E. Pinel, M. Oubaha, R. Mahiou, E. Cavalli, M. Bettinelli, Opt. Mater. **28**, 9 (2006).

[4] W. A. Pisarski, J. Mol. Struct. **744-747**, 473 (2005).

[5] B. Chen, J. Xu, H. Liang, Z. Zheng, Q. Zhang, J. Optoelectron. Adv. Mater. **7**(6), 2991 (2005).

[6] M. S. Iovu, A. M. Andries, S. A. Buzurniuc, V. I. Verlan, E. P. Colomeico, St.V. Robu, J. Optoelectron. Adv. Mater. **8**(1), 257 (2006).

[7] A. Florez, O. L. Malta, Y. Messaddeq, M. A. Aegerter, J. Non-Cryst. Solids **213-214**, 315 (1997).

[8] E. Meneses-Macheco, C. B. de Araujo, Y. Messaddeq, J. Non-Cryst. Solids **226**, 265 (1998).

[9] E. Pecoraro, D. F.de Sousa, R. Lebullenger, A. C. Hernandes, L. A. O. Nunes, J. Appl. Phys. **86**, 3144 (1999).

[10] L. E. E. de Araujo, A. S. L. Gomes, C. B. de Araujo, Y. Messaddeq, A. Florez, M. A. Aegerter, Phys. Rev. B **50**, 16219 (1994).

[11] B. W. Lozano, C. B. de Araujo, C. Egalon, A. S. L. Gomes, B.J. Costa, Y. Messaddeq, Optics Commun. **153**, 271 (1998).

[12] M. B. Saisudha, J. Ramakrishna, Phys. Rev. B **53**, 6186 (1996).

[13] M. B. Saisudha, K. S. R. Koteswara Rao, H. L. Bhat, J. Ramakrishna, J. Appl. Phys. **80**, 4845 (1996).

[14] M. R. Reddy, S. B. Raju, N. Veeraiah, J. Phys. Chem. Solids **61**, 1567 (2000).

[15] B. Karthikeyan, S. Mohan, Physica B **334**, 298 (2003).

[16] B. Karthikeyan, Reji Philip, S. Mohan, Opt. Commun. **246**, 153 (2005).

[17] A. Boutarfaia, M. Poulain, Solid State Ionics **144**, 117 (2001).

[18] A. Boutarfaia, M. Legouera, M. Poulain, J. Non-Cryst. Solids **291**, 176 (2001).

[19] W. A. Pisarski, J. Pisarska, W. Ryba-Romanowski, Chem. Phys. Lett. **380**, 604 (2003).

[20] B. Karmakar, P. Kundu, R. N. Dwivedi, Mater. Lett. **57**, 953 (2002).

[21] A. S. Oliveira, E. A. Gouveia, M. T. de Araujo, A. S. Gouveia-Neto, C. B. de Araujo, Y. Messaddeq, J. Appl. Phys. **87**, 4274 (2000).

[22] G. Lakshminarayana, S. Buddhudu, Physica B **373**, 100 (2006).

[23] A. G. Souza Filho, J. Mendes Filho, F. E. A. Melo, M. C. C. Custodio, R. Lebullenger, A. C. Hernandes, J. Phys. Chem. Solids **61**, 1535 (2000)

[24] M. Shojiya, Y. Kawamoto, K. Kadano, J. Appl. Phys. **89**, 4944 (2001).

[25] Z. Mazurak, W. A. Pisarski, J. Pisarska, M. Żelechower, Phys. Stat. Sol.(b) **237**, 581 (2003).

[26] W. A. Pisarski, J. Pisarska, G. Dominiak-Dzik, W. Ryba-Romanowski, J. Phys.: Condens. Matter **16**, 6171 (2004).

[27] B. R. Judd, Phys. Rev. **127**, 750 (1962).

[28] G. S. Ofelt, J. Chem. Phys. **37**, 511 (1962).

[29] M. Malinowski, M. Kowalska, R. Piramidowicz, T. Łukasiewicz, M. Świrkowicz, A. Majchrowski, J. Alloys Comp. **323-324**, 214 (2001).

[*]Corresponding author: wpisarsk@us.edu.pl